NH_2-MIL-53(AL) AND NH_2-MIL-101(AL) IN SULFUR-CONTAINING COPOLYIMIDE MIXED MATRIX MEMBRANES FOR GAS SEPARATION

Beatriz Seoane[1], Carlos Téllez[1*], Joaquín Coronas[1] and Claudia Staudt[2]

[1]Department of Chemical and Environmental Engineering and Instituto de Nanociencia de Aragón (INA), Universidad de Zaragoza, 50018 Zaragoza, Spain

[2]BASF SE, GMM/M - B001, 67056 Ludwigshafen, Germany

*To whom correspondence should be addressed: e-mail: ctellez@unizar.es; Tel.: +34 976 762897; Fax: +34 976 76 1879.

ABSTRACT

Amino functionalized MOFs (NH_2-MIL-53(Al) or NH_2-MIL-101(Al)) were used as dispersed phase in the fabrication of mixed matrix membranes (MMMs) with a polymer matrix of sulfur-containing copolyimides (6FDA:DSDA/4MPD:4,4'-SDA 1:1 (polymer P1) or 6FDA/4MPD:4,4'-SDA 1:1 (polymer P2)). The gas separation properties of the MMMs obtained were tested for permeation of H_2, CH_4 and CO_2. Membranes comprising polymer P1 showed better interaction with the fillers used than polymer P2, and therefore better separation properties, especially for NH_2-MIL-101(Al). Upon NH_2-MIL-101(Al) loading the performance of pure polymer was improved approaching the Robeson 1991 H_2/CH_4 and CO_2/CH_4 upper bound limits with high permeabilities, e.g. 114, 71 and 1.7 Barrer for H_2, CO_2 and CH_4, respectively, using 10 wt.% NH_2-MIL-101(Al)@P1. These improvements are related to the pore size of the filler, the flexibility and functional groups of sulfone-containing DSDA, and polymer rigidification.

Keywords: ***Metal–organic framework, NH_2-MIL-53(Al), NH_2-MIL-101(Al), Mixed-matrix membrane, Gas separation***

1. Introduction

Although nowadays gas separation on an industrial scale is mainly carried out by means of distillation, low temperature condensation or adsorption processes, membrane technology is a promising method in economic and energy saving terms [1]. While ceramic or inorganic membranes may have applications in special cases due to their good permselectivity and high thermal and chemical stability, the majority of membrane based gas separation industrial processes use polymeric membranes because of their easy processability and low cost [2].

As Robeson reported in 1991 [3] (updated in 2008 [4]), there is a trade-off between permeability and selectivity in the separation of gas mixtures by polymers. In recent years several approaches have been developed to overcome this limitation. One approach is fabricating so-called mixed matrix membranes (MMMs) which consist of a composite comprising two phases: a polymer matrix and a dispersed phase [5]. The first MMMs were prepared using conventional fillers such as zeolites, carbon molecular sieves and silicas. However, over the last few years new materials have been incorporated, e. g. carbon nanotubes, clay layered silicates, metal organic frameworks (MOFs) or graphene [2,6,7].

MOFs have important advantages when compared with other fillers. One of the main problems of zeolite based MMMs is the formation of voids at the interface because of the poor affinity between the inorganic and the organic phase, thus lowering the selectivity of the membrane and therefore causing it to underperform [8]. However, in the case of MOFs the organic ligand may improve the filler-polymer interaction [9,10], avoiding the presence of non-selective micro gaps.

Since the first pioneering work of Yehia et al. [11] based on the use of Cu BPDC-TED to improve selectivity for CH_4, several MOF based MMMs have been reported and

recently the subject has been reviewed [7, 12, 13]. Membranes of highly permeable polyimide, specifically 6FDA/DAM, containing ZIF-90 showed an unprecedented high performance for CO_2/CH_4 separation and promising CO_2/N_2 separation properties [14]. As a different approach, the use of flexible fillers such as NH_2-MIL-53(Al) with different polymers such as polysulfone or polyimide enable the fabrication of MMMs whose selectivities are enhanced at high pressures [15,16]. NH_2-MIL-53(Al) shows excellent adhesion with these polymers, allowing loadings up to 32 wt.%. More recently, Nik et al. [17] prepared MMMs composed of UiO-66, NH_2-UiO-66, UiO-67, MOF-199 or NH_2-MOF-199 with 6FDA-ODA. They reported that fillers containing amino groups may improve the interaction between the polymer matrix and the dispersed phase, and may lead to the rigidification of the polymer at the interface of both phases, decreasing the permeability while increasing the selectivity.

NH_2-MIL-53(Al), first reported by Arstad et al. [18], is based on MIL-53 topology, where 1,4-benzenedicarboxylic acid is replaced by 2-aminoterephthalic acid. MIL-53 exhibits 1D diamond-shaped channels and is built from chains of $(AlO_4(OH)_2)$ corner-sharing octahedra, which are connected by means of the organic ligand [19]. The empirical formula of NH_2-MIL-53(Al) is $Al(OH)[H_2N\text{-}BDC]\cdot 0.9H_2O$ [20]. Although MIL-53 and NH_2-MIL-53 exhibit the same topology, their so-called breathing behavior is different. Whereas, upon dehydration, MIL-53 has open pores of diameter 8.5 Å at room temperature (large pore form, lp), NH_2-MIL-53(Al) has a very narrow pore form (vnp form) because of the hydrogen bonding between the NH_2 groups of the organic ligand and the bridging oxygen atoms and OH groups of the infinite corner-sharing chains [21]. MIL-101 has been reported to be the kinetically favored form of MIL-53 [22]. MIL-101 is composed of trimeric metal octahedral units that are interconnected by the organic linker to form supertetrahedra (STs). The STs are further connected to each

other to obtain the augmented MTN-type zeolite framework. This topology exhibits two types of cages: small cages, which possess a free diameter of 29 Å and pentagonal windows of 12 Å, and larger cages with a free diameter of 34 Å and both pentagonal and hexagonal windows, the latter with a 14.5 Å by 16 Å free aperture [23,24]. The empirical formula of MIL-101 synthetized with chromium as metal and fluorhydric acid is $Cr_3F(H_2O)_2O[BDC]_3 \cdot nH_2O$ [23].

Fluorinated sulfur-containing copolyimides have recently been reported to show high potential for optical applications [25]. In this work we have studied the gas permeation properties of the tioether and sulfone-containing copolyimides 6FDA:DSDA/4MPD:4,4'-SDA (1:1) and 6FDA/4MPD:4,4'-SDA for the first time, and we have prepared MMMs with NH_2-MIL-53(Al) and NH_2-MIL-101(Al). The aim was to study the influence of the functional groups of the polymer on the interaction between the copolyimide and the MOF materials which could affect the overall performance of the membrane in gas separation.

2. Experimental

2.1. Synthesis of NH_2-MIL-53(Al)

NH_2-MIL-53(Al) synthesis was carried out under the optimized synthesis conditions previously reported by Ahnfeldt et al. [20]. In a typical synthesis, 3.1 g of $Al(NO_3)_3 \cdot 9H_2O$ (Sigma Aldrich, ≥98%) was mixed with 1.5 g of 2-aminoterephthalic acid (NH_2-H_2BDC, Sigma Aldrich, 99%) in a Teflon®-lined autoclave. Then 22.8 mL of distilled water was added and the mixture was heated up to 150 ºC for 5 h. The product obtained was washed 3 times with acetone. NH_2-MIL-53(Al) was activated in order to remove the unreacted NH_2-H_2BDC present in the pores. For this purpose, as-synthesized NH_2-MIL-53(Al) was treated at 150 ºC for 48 h in N, N-

dimethylformamide (DMF, Alfa Aesar, 99%) and then the powder was evacuated heated at 150 ºC for 8 h to remove the trapped DMF.

2.2. Synthesis of NH_2-MIL-101(Al)

The procedure followed to obtain NH_2-MIL-101(Al) was performed as described by Serra-Crespo et al. [24]. In this case 0.51 g of $AlCl_3 \cdot 6H_2O$ (Sigma Aldrich, 99%) and 0.56 g of NH_2-H_2BDC were dissolved in 30 mL of DMF. After 30 min stirring the autoclave was capped and heated at 130 ºC for 3 days. Then the product was washed 3 times with acetone. As-synthesized NH_2-MIL-101(Al) was activated with methanol under reflux overnight and evacuated at 200 ºC for 16 h.

2.3. Copolyimide synthesis

The monomers used for copolyimide synthesis (see structure in Fig. 1) - 4,4'-(hexafluoroisopropylidene) diphthalic anhydride (6FDA, Alfa Aesar, 99%), 3,3',4,4'-diphenylsulfonetetracarboxylic dianydride (DSDA, TCI, >96%), 2,3,5,6 tetramethyl-p-phenylenediamine (4MPD, Sigma Aldrich, 99%) and bis(4-aminophenyl) sulfide (4,4'-SDA, TCI, >98%) - were purified by sublimation prior to their use. Besides, dimethylacetamide (DMAc, Merk, for synthesis) was distilled before use as a solvent, and acetic anhydride (Acros Organics, >99%) and triethylamine (Acros Organics, >99%) were used as received.

In order to study the influence of the polymer composition on the interaction between MOFs and the polymer in the MMMs, a mixture 1:1 of the diamines 4MPD and 4,4'-SDA was polymerized with two different dianhydrides: a mixture 1:1 of 6FDA with DSDA (hereafter polymer 1, P1) and 6FDA (hereafter polymer 2, P2).

To obtain the copolyimides, a two-step procedure was followed [26]. In the first step the diamines were dissolved in DMAc in a moisture free flask under nitrogen atmosphere and 6FDA was added in small portions. Then the mixture was stirred overnight and

polyamic acid (PAA) was formed. In the second step PAA was chemically imidized using an equimolar, threefold excess (based on the total amount of diamine monomers) of a triethylamine/acetic anhydride mixture, and the mixture was heated up to 120 ºC for 30 min. After cooling, the product was precipitated in a 1:1 volume mixture of ethanol and distilled water. The polymer was milled and washed with ethanol before drying at 150 ºC for 48 h under vacuum.

2.4. Preparation of MOF mixed matrix membranes

First of all, bare P1 and P2 membranes were prepared in order to compare their results with those of MMMs. These MOF – free membranes were obtained preparing a solution of P1 or P2 (0.3 g) in THF (Sigma – Aldrich) which was filtered through a syringe filter (PTFE membrane, 0.45 μm pore size). The percentage of the solvent was 95 wt.%, selected to assure a good viscosity of the casting solution. This percentage was maintained for the fabrication of the MMMs.

MMMs containing nominal loadings of 10 and 15 wt.% of activated NH_2-MIL-53(Al) and 5 and 10 wt.% of activated NH_2-MIL-101(Al) were prepared. The preparation of the MOF filled copolyimide membranes was identical to the preparation of the bare membranes, but after filtering the polymer solution, the filler was added to the solution and dispersed in an ultrasonic bath for 30 min. Then the casting solution was stirred overnight. The suspensions obtained were sonicated three times for 15 min. Subsequently, the membranes were cast into metal rings of 9 cm in diameter. These were placed on a glass surface and covered with a funnel to slow down the natural evaporation of solvent under ambient conditions. The final step consisted in removing the remaining solvent under vacuum conditions at 150 ºC for 24 h.

2.5. Characterization

X-Ray diffraction (XRD). XRD was performed at room temperature using a D-Max Rigaku diffractometer with a copper anode and a graphite monochoromator to select Cu-$K_{\alpha 1}$ radiation (λ = 1.5418 Å). Data were collected between 2θ = 2.5-40º and the scanning rate used was 0.03 º/s.

Scanning Electron Microscopy (SEM). SEM images were acquired with an Inspect F scanning electron microscope (FEI) operating at 10 kV. Cross sections of mixed matrix membranes were prepared by freeze-fracturing after immersion in liquid N_2.

N_2 adsorption. Data were collected at 77 K on an Micrometrics ASAP 2020 V1.04 H. NH_2-MIL-53(Al) was outgassed at 130 ºC for 10 h and NH_2-MIL-101(Al) was outgassed at 200 ºC for 16 h prior to the measurements. The selected heating rate was 1 ºC/min.

Thermogravimetric analysis (TGA): TGA experiments were performed using a TGA/SDTA 851e system (Mettler Toledo AG). The samples were heated up to 850 ºC with a heating rate of 10 ºC/min under an air flow of 80 cm^3(STP)/min.

Differential Scanning Calorimetry (DSC). DSC was acquired with a Mettler Toledo DSC822^e. The samples were first scanned from 30 to 200 ºC at a heating rate of 10 ºC/min and then three consecutive runs from 30 to 400 ºC at 20 ºC/min. The glass transition temperature (T_g) value was taken from the middle point of the slope transition in the DSC curve as an average value based on the second and third run for a minimum of three samples.

Infrared Spectroscopy (FTIR). Attenuated total internal reflection Fourier (ATR-FTIR) spectroscopy was performed using a Bruker Vertex 70 FTIR spectrometer. Spectra were recorded averaging 40 scans in the 4000 – 600 cm^{-1} wavenumber range with a resolution of 4 cm^{-1}.

Gas Permeation Measurements. To determine the H_2, CH_4 and CO_2 permeabilities of the MMMs, a constant-volume/variable-pressure apparatus was used [26]. In this system, the membranes were placed in a stainless steel permeation cell that separates two cylindrical volumes, each one equipped with a pressure transducer. After degassing the whole equipment for several hours, the valve connecting the system with the vacuum pump was closed and the upstream volume was pressurized with single gas up to 3 bar. When the membrane starts to permeate, the pressure increases in the downstream volume (65 mL), and this increase in pressure with time was recorded. In order to obtain more reliable results [27], the collected data were corrected with the leak rate obtained in a leakage test performed prior to the measurements. This procedure was repeated three times for each membrane and each gas. The permeability was calculated from the steady state slope of three different membranes for each condition. The ideal selectivity was calculated as the ratio of experimental permeabilities.

3. Results and discussion

3.1. Synthesis and characterization of NH_2-MIL-53 and NH_2-MIL-101

XRD patterns of as-synthesized NH_2-MIL-53(Al) and NH_2-MIL-101(Al) matched well with the previously reported diffraction data and indicated that pure phases were obtained (see Fig. 2) [20,24]. It is known that peak signals of NH_2-MIL-53 change depending on the guest molecules inside the pores because of the breathing effect. The two first peaks at 8.7 and 10.4° indicated that the pattern corresponded to the as-synthesized NH_2-MIL-53(Al), in which unreacted NH_2-H_2BDC was trapped in the structure [20]. DMF has been reported to stabilize MOF-235 as a precursor of NH_2-MIL-101(Al), and the presence of moisture is known to accelerate the decomposition of the latter over time [22]. Therefore, when replacing H_2O by DMF and $Al(NO_3)_3 \cdot 9H_2O$

by $AlCl_3 \cdot 6H_2O$ (a less hydrated salt), the diffraction changed and new peaks appeared at lower 2θ, indicating the formation of the less thermodynamically favorable phase NH_2-MIL-101(Al). In addition, SEM images (Fig. 3) showed that the NH_2-MIL-101(Al) particles were smaller (104 ± 28 nm) and more aggregated than the NH_2-MIL-53(Al) crystals (358 ± 138 nm), both particle sizes obtained from about 50 particles measured from several SEM images.

As has been indicated in the experimental section, as-synthesized NH_2-MIL-53(Al) and NH_2-MIL-101(Al) were activated in order to remove unreacted ligand or/and DMF. The absence of signals in the 1673-1690 cm^{-1} range in the FTIR spectrum of activated NH_2-MIL-53, assigned to the C=O stretching vibration of the carboxylic group of unreacted NH_2-H_2BDC and the C=O stretching vibration of amide group of the DMF, respectively, indicated that the NH_2-MIL-53 was well activated (Fig. 4). In the activated NH_2-MIL-101 spectrum it is possible to detect the presence of residual amounts of DMF; nevertheless, nitrogen adsorption shows that this material was effectively activated.

The thermogravimetric analysis of activated NH_2-MIL-53(Al) (Fig. 5a) showed a weight loss of 6.7 % up to 120 ºC. This loss has been reported by Ahnfeldt et al. [20] to be due to the release of water molecules trapped in the pores of the structure. As expected, the introduction of the amino group in the organic ligand decreased thermal stability from 500 ºC for MIL-53(Al) to 420 ºC for NH_2-MIL-53(Al). In fact at 420 ºC, the thermogravimetric analysis shows the starting of a weight loss mainly related to the organic ligand. The final residue of 22.1 % corresponded to Al_2O_3. In the case of NH_2-MIL-101 (Fig. 5a), the thermal stability was slightly lower than that of NH_2-MIL-53(Al) and the material started to decompose at 370 ºC. This behavior is similar to that reported for MIL-53(Cr) and MIL-101(Cr). The former is stable up to 375 ºC [28],

while the stability of the latter decreases up to 275 ºC [23]. In NH_2-MIL-101, water release (2.7 %) was followed by desorption of some DMF, according to the FTIR analysis, and the final residue of 24.6 % corresponded to Al_2O_3.

Finally, nitrogen adsorption was performed in activated samples. NH_2-MIL-53(Al) pores were not open until P/P_0 does not reach a value of approximately 0.3 due to diffusion limitations (Fig. 5b) and, therefore, the BET surface was not calculated. It was also observed that, as has already been reported [20], the N_2 isotherm of NH_2-MIL-53(Al) showed hysteresis behavior and there was no desorption. The BET area of NH_2-MIL-101(Al) calculated between P/P_0 0.03–0.15 according to Snurr's [29] criteria was 1968 m^2/g, which was in accordance with the previously reported value [24].

3.2. Preparation and characterization of MMMs

The dispersion of the filler in the polymer matrix was good for both NH_2-MIL-53(Al) and NH_2-MIL-101(Al) with both polymers P1 and P2 (Figs. 3c-f). In the case of NH_2-MIL-101(Al), aggregates observed in the powder were broken and well dispersed during the membrane preparation by means of ultrasound treatment, and the interaction was better than using NH_2-MIL-53(Al). This may be due to its smaller particle size or to a larger pore aperture that allows migration of the polymer chains into the cavities, as has been already observed by Ren et al. [30] for MOF-5@PMDA/ODA membranes. Besides, a crater morphology was observed which showed polymer veins around the particles. This has been previously reported and attributed to interfacial stress indicating good interaction between the MOF and the polymer [31,32]. Interestingly, as discussed below, adhesion between NH_2-MIL-53(Al) and P1 was better than the adhesion with P2 which showed non-selective voids (see inset of Fig. 3e) that degraded the membrane performance.

From the TGA curves, and taking into account the formulae for both MOFs, the experimental MOF loading could be calculated. This matched well with the theoretical values (see Table 1). Chen et al. [16] reported that the DGT peak of pure polymer was shifted to higher temperatures as MOF loading increased. This behavior can also be observed in Fig. 6a which shows that the DGT peak of P1 appeared at higher temperatures upon MOF loading (from 583 ºC to 589 ºC for 10 wt.% NH_2-MIL-53(Al)@P1 and from 583 ºC to 590 ºC for 10 wt.% NH_2-MIL-101(Al)@P1 MMMs). However, the DTG peak remained unchanged for MMMs of polymer P2 (Fig. 6b), in the case of NH_2-MIL-53 filler probably because of the worse interaction as Fig. 3e suggests. A similar trend was observed for the glass transition temperature (Table 1). An increase in MOF loading in P1 resulted in higher T_g while its value remained unchanged for MMMs prepared with P2. The increase of T_g with filler loading in the MMM may be related to the rigidification of the polymer chains which surround the MOF particles. This effect was less pronounced for NH_2-MIL-53(Al) than for NH_2-MIL-101(Al), with an increase of T_g from 360 to 363 ºC upon 10 wt.% loading for the former, and from 360 to 366 upon 10 wt.% loading for the latter. In fact, we were unable to prepare MMMs with P1 polymer whose loadings were higher than 15 wt.% for NH_2-MIL-53(Al) and higher than 10 wt.% for NH_2-MIL-101(Al) as they became brittle, and it was not possible to carry out the permeation experiments. As expected, pure polymers exhibited high T_g since polymer containing 4MPD and 6FDA show glass transition temperatures higher than 400 ºC [33]. P1 and P2 polymers showed lower T_g because they contained two diamines: 4MPD and also 4,4'-SDA in a ratio of 1:1. 4MPD hampers the rotation of the single bonds, making the polymer chain stiffer and therefore the T_g higher. When 4MPD units are replaced by 4,4'-SDA, T_g decreases [33]. In addition, when part of the 6FDA monomer was replaced by DSDA, the T_g decreased

slightly since DSDA units give a relatively higher flexibility to the polymer backbone than the 6FDA units [34]. This flexibility of DSDA would allow better polymer chain penetration in the pores, consistent with the better interaction observed for P1 compared to P2.

Figs. 7 and 8 show the FTIR spectra for MMMs between 1800 and 1000 cm^{-1} and 3800 and 3200 cm^{-1}, respectively. For pure polymer, absorption bands at 1785, 1718, 1351 and 719 cm^{-1} corresponded to asymmetric and symmetric C=O stretching, C-N stretching and imide five-ring deformation [25]. Besides, the signal at 1327 cm^{-1} was related to the asymmetric stretching of SO_2 [35]. In the case of pure MOFs, NH_2-MIL-53(Al) and NH_2-MIL-101(Al) bands at 3504 and 3391 cm^{-1} and the shoulder at 1624 cm^{-1} corresponded to the asymmetric and symmetric amine stretching and the N-H scissoring vibration, thus confirming the presence of amino groups in the framework [20,24].

The good affinity between P1 and amine functionalized MOFs may be due to the formation of hydrogen bonds between the carboxylic groups of the pure polymer with the amine groups of the fillers, since these bands are shifted in the FTIR spectra as has been noted in other MMMs with MOFs [16,17]. The carboxyl band υ(C=O) of P1 was slightly shifted from 1717 cm^{-1} to 1720 cm^{-1} for 10 wt.% NH_2-MIL-53(Al)@P1 and from 1717 cm^{-1} to 1721 cm^{-1} for NH_2-MIL-101(Al)@P1, while υ_{as}(N-H) and υ_{s}(N-H) of NH_2-MIL-53(Al) were slightly shifted from 3503 to 3500 cm^{-1} and from 3391 to 3389 cm^{-1}, respectively. In the case of 10 wt.% NH_2-MIL-101(Al)@P1 υ_{as}(N-H) and υ_{s}(N-H) bands of NH_2-MIL-101(Al) were shifted from 3505 to 3495 cm^{-1} and from 3391 to 3389 cm^{-1}, respectively, suggesting the formation of hydrogen bonds between the carboxylic group of polymer P1 and amino groups of the fillers. The shift of the NH_2-MIL-101(Al) amine groups was slightly larger than that observed for NH_2-MIL-53(Al),

consistent with the fact that for the former the affinity and contact with the polymer was better. Signal at 1327 cm^{-1} related to the asymmetric stretching of SO_2 was not shifted indicating that there is no interaction of the MOFs with this group. It should be noted that some shifts are of the same order as the resolution of the FTIR, however in P2 the absorption signal in FTIR was not shifted (not shown).

3.3. Permeation results

Permeation results for CO_2/CH_4 and H_2/CH_4 are shown in Figs. 9 and 10. P1 was less permeable but more selective for CO_2 and H_2 than P2. The higher permeability of P2 was due to the higher content of 6FDA dianhydride. This dianhydride possesses bulky -CF_3- side groups that improve the free volume of the polymer, which increases the permeability of the copolyimide [36]. Besides, the presence of sulfonyl groups has been reported to increase selectivity [37].

According to the permeation data, the performance of MMMs fabricated with P2 membranes was worse than that of P1 membranes since for the former the selectivity was decreased upon 10 wt.% NH_2-MIL-53(Al) loading, while for the latter it was slightly increased, thus indicating the presence of non-selective voids when P2 was used.

The interaction between amino functionalized MOFs and P1 was shown to be good not only by the SEM images and FTIR spectra, but also the permeation results. 10wt.% NH_2-MIL-53(Al) MMMs scars show improvements with respect to pure polymer. Upon 15wt.% NH_2-MIL-53(Al)@P1 loading both permeation and ideal selectivities were slightly increased (Table 2). Despite the fact that at higher loading the membrane performance has been reported [16] to improve (up to 32 wt.%) due to the selective adsorption of CO_2, as previously remarked we were not able to prepare membranes with

more than 15 wt.%. At higher loadings the membrane became brittle and it was not possible to fix it in the permeation module without breaking.

Regarding the bare polymer, the improvements are more marked with NH_2-MIL-101(Al), especially with polymer P1 (Figs. 9 and 10). For NH_2-MIL-101(Al)@P1, increasing MOF loading up to 10 wt.% resulted in a P_{CO2} increase of 22%, from 57.9 up to 70.9 Barrer, and a 27 % P_{H2} increase, from 90.1 to 114.1 Barrer. In fact, it has recently been reported that NH_2-MIL-53(Al) membranes exhibit very high permeance for H_2 [38], and the permeance of NH_2-MIL-101(Al) is expected to be even higher due to its larger pore size. This trend is similar to that previously reported by Tanh Jeazet et al. [39], who observed that P_{O2} could be increased by a factor of four for 24% MIL-101(Cr)@PSF MMMs. In our case this effect was less pronounced because of the rigidification of the polymer matrix with MOF loading, leading to a decrease in the permeability of the MMM. Since the CO_2/CH_4 selectivity of NH_2-MIL-101(Al) has been reported [24,40] to be lower than that of NH_2-MIL-53(Al), the increase upon 10 wt.% NH_2-MIL-101(Al) may also be due to the rigidification of the polymer chains around the filler particles. As previously discussed this rigidification effect was larger for NH_2-MIL-101(Al) than for NH_2-MIL-53(Al), probably due to the better accessibility to the amino groups present in the pores and to the smaller particle size. To study the effect of polymer rigidification with NH_2-MIL-101(Al), a mixed matrix membrane with 5 wt% loading was prepared. As shown in Table 2, the permeability decreased 9.1% for CO_2 and 6.8% for H_2 and the ideal selectivities increased. This is in accordance with the behavior observed for MMMs in which polymer chains surrounding filler particles are rigidified, e. g. MOF-5, MIL-53 or NH_2-UiO-66 and different polyimides [17,30]. In summary, rigidification (permeability decreases and selectivity increases) predominates upon 5 wt.% NH_2-MIL-101(Al) loading, and the permeability properties of the filler

have influence upon 10 wt.% NH_2-MIL-101(Al) loading even though some small voids could explain part of the increase in permeability when the loading increases.

Finally, our results are compared with those found in the literature (Fig. 11 and Table 3). As previously discussed, Bae et al. [14] prepared high-performance membranes composed of 15wt.% ZIF-90 and 6FDA/DAM copolyimide. These membranes had unprecedented high performance for CO_2/CH_4, lying far above the 1991 upper bound, as shown at point H in Fig. 11a. Besides, Nik et al. [17] and Chen et al. [16] used amino-functionalized MOFs, such as NH_2-MIL-53(Al) and NH_2-MOF-199, and non-functionalized MOFs such as UiO-66. With these fillers and using 6FDA/ODA as the polymer matrix they were able to reach the 1991 upper bound for 32 wt.% NH_2-MIL-53@6FDA/ODA (M), 25 wt.% NH_2-MOF-199@6FDA/ODA (L2) and 25 wt.% UiO-66@6FDA/ODA (L1) MMMs, demonstrating that these fillers are promising for the separation of CO_2/CH_4 mixtures. As a different approach MOF-5 has been used to increase pure polymer permeability [32]. The performance of Matrimid® was improved upon MOF-5 loading. For 30 wt.% MOF-5@Matrimid® MMMs, H_2 permeability increased up to 120% without any loss of selectivity (E). For membranes prepared with a loading of 20 wt.% (A), the increase of permeability was even higher (247%) and only a slight decrease in selectivity (7.3%) was observed, which may be due to the presence of non-selective voids. Besides, the different behavior of A and E, both using Matrimid® 5218 as polymer matrix and MOF-5 as dispersed phase, may be due to the different operation conditions: 50 ºC and 7 bar for the former and 35 ºC and 2 bar for the latter. When our results are compared to the results reported for other MMMs prepared with MOFs, and taking into account that membranes with high permeability and moderate selectivity may be industrially more attractive, it can be seen that the performance of our membranes is among the best published so far. For instance, 10

wt.% NH_2-MIL-101(Al)@P1 membranes (Z1) exhibited the best behavior, being on the 1991 upper bound for both H_2/CH_4 and CO_2/CH_4 mixtures. MMMs made with P2 show slightly worse results than pure polymer P2 due to the poor affinity between the amino-functionalized filler and the polymer matrix. This effect was more pronounced for NH_2-MIL-53(Al) than for NH_2-MIL-101(Al) due to the formation of non-selective voids that lowered the selectivity. Using highly permeable polymers and tuning their functional groups to improve their affinity and contact with the filler has made it possible to improve the behavior of the pure polymer.

4. Conclusions

In this work, MMMs composed of sulfur-containing copolyimides (named P1 and P2) and amino-functionalized MOFs (NH_2-MIL-53(Al) and NH_2-MIL-101(Al)) have been prepared and tested for permeation of H_2, CO_2 and CH_4. The main difference between the polymers is that in P1 part of the 6FDA dianhydride with the group CF_3 has been substituted by the more flexible DSDA dianhydride with the group $–SO_2$. Both polymers showed different degrees of contact for the dispersed phase (better for polymer P1 than for polymer P2), thus indicating that the functional groups and the flexibility of the polymers had an influence on the filler-polymer matrix interphase and, therefore, on the overall performance of the membranes.

Upon MOF loading in P1, T_g was increased. This was related to the rigidification of the polymer matrix when MOF was added, due to the high affinity between both phases. This effect was less pronounced for NH_2-MIL-53(Al) than for NH_2-MIL-101(Al), due to the larger pore aperture of MIL-101 which allows greater accessibility to the functional groups. This rigidification of the polymer was also indicated by the fact that when low loadings were used, the MMM gas permeabilities decreased. 10 wt.% NH_2-

MIL-101(Al) MMMs showed the best performance. MOF loading improved the behavior of the pure polymer, approaching the 1991 upper bound and being among the best results reported to date.

Acknowledgments

The authors gratefully acknowledge the Spanish Ministry of Economy and Competitiveness (MINECO) for financial support through project MAT2010-15870, as well as the Regional Government of Aragón (DGA) and the European Social Fund (ESF). B.S. acknowledges a grant from the MINECO (FPU Program).

Table 1. Calculated wt. % loading from TGA curves according to the empirical formula and glass transition temperature (T_g) of the MMMs prepared.

	MOF loading [wt. %]			T_g (ºC)	
	Nominal	Polymer P1 (TGA)	Polymer P2 (TGA)	Polymer P1	Polymer P2
Bare polymer	0	--	--	360 ± 1.0	354.6 ± 1.8
NH_2-MIL-53(Al)	5	--	--	362.6 ± 0.1	-
	10	9.7	10.2	363.4 ± 0.7	354.7 ± 4.6
	15	14.5	--	363.1 ± 1.0	-
NH_2-MIL-101(Al)	5	6.4		360.5 ± 0.3	-
	10	11.2	9.7	366.3 ± 0.5	352.7 ± 1.1

Table 2. H_2, CH_4 and CO_2 permeability and P_{H2}/P_{CH4} and P_{CO2}/P_{CH4} ideal selectivity at 35 ºC and 3 bar.

Sample	wt.%	Permeability (Barrer)			P_{H2}/P_{CH4}	P_{CO2}/P_{CH4}
		H_2	CH_4	CO_2		
P1	0	90.1±1.9	1.6±0.1	57.9±3.3	54.7±1.0	35.1±1.3
NH_2-MIL-53@P1	10	89.5±3.8	1.6±0.1	56.9±5.1	56.4±1.2	35.8±1.0
	15	100±3	1.8±0.1	66.5±4.2	55.8±1.0	36.9±0.4
NH_2-MIL-101@P1	5	84.0±1.8	1.2±0.1	52.6±4.4	67.3±0.7	42.2±0.5
	10	114±2	1.7±0.2	70.9±4.1	68.0±2.0	41.6±1.8
P2	0	169±3	4.5±0.3	134±1	38.0±1.8	30.2±1.8
NH_2-MIL-53@P2	10	175±4	5.0±0.2	137±2	34.7±2.1	27.2±0.9
NH_2-MIL-101@P2	10	191±5	5.1±0.4	151±5	37.6±1.5	29.6±1.2

Table 3. CO_2/CH_4 and H_2/CH_4 separation data for selected MOF based MMMs reported in literature.

MOF	Loading (wt.%)	Polymer	Operating conditions			Figs. 11 code	Ref	P_{CO2} [Barrer]	P_{CO2}/P_{CH4} [-]	P_{H2} [Barrer]	P_{H2}/P_{CH4} [-]
			Analysis	T [ºC]	ΔP [bar]						
IRMOF-1	20	Matrimid®	Single gas	50	7	A	[41]	38.8	29.2	115	86.4
$[Cu_2(PF_6)(NO_3)(4,4'\text{-bby})_4]\cdot 2PF_6\cdot 2H_2O$	5	PSF	Single gas	35	1	B	[42]	-	-	9.8	200
HKUST-1	30	PDMS	-	-	-	C1	[43]	2900	3.7	-	-
	5	PSF				C2		7.7	21.5	11.3	32
CU-BPY-HFS	10	Matrimid®	Single gas	35	2.7	D1	[31]	7.8	31.9	16.9	69.2
	30					D2		10.4	27.5	20.3	53.9
MOF-5	30	Matrimid®	Single gas	35	2	E	[32]	20.2	44.7	53.8	120
CuTPA	15	PVAc	Single gas	35	4.5(0.1 for CO_2)	F	[27]	3.3	40.4	-	-
ZIF-8	50	Matrimid®	Single gas	35	2.7	G	[44]	4.7	125	18.1	472
ZIF-90	15	6FDA/DAM	Single gas	25	2	H	[14]	800	26.6	-	-
NH_2-MIL-53(Al)	25	PSF	Mixture (1:1)	-10	10	I	[15]	2.4	117	-	-
ZIF-8	16	PSF	Mixture (1:1)	35	2	J	[45]	12.1	19.8	39.8	117.8
ZIF-8	30	PEES	Single gas	-	-	K	[46]	50	20.8	91	37.9
$[Cu_3(BTC)_2]$	30	Matrimid®	Mixture (35:65)	35	5	-	[47]	0.65*	33.0	-	-
ZIF-8								0.68*	31.5	-	-
MIL-53(Al)								0.71*	32.0	-	-
UiO-66	25	6FDA/ODA	Single gas	35	10	L1	[17]	50.4	46.1	-	-
NH_2-MOF-199	25					L2		26.6	59.6		
NH_2-MIL-53(Al)	32	6FDA/ODA	Single gas	35	10	M	[16]	14.6	78	-	-
NH_2-MIL-101(Al)	10	P1	Single gas	35	3	Z1	This work	70.9	41.6	114	68.0
		P2				Z2	This work	150	29.6	191	37.6

* P_{CO2} units GPU.

FIGURE CAPTIONS

Figure 1. Monomers used for the copolyimide synthesis.

Figure 2. XRD patterns of as–synthesized NH_2-MIL-53(Al) and NH_2-MIL-101(Al). Simulated NH_2-MIL-53(Al) and NH_2-MIL-101(Cr) has been added for comparison. The XRD patterns were simulated using the software Mercury from the lattice parameters obtained from the Cambridge Structural Database.

Figure 3. SEM images of a) as–synthesized NH_2-MIL-53(Al), b) as–synthesized NH_2-MIL-101(Al), c) 10 wt.% NH_2-MIL-53(Al)@P1, d) 10 wt.% NH_2-MIL-101(Al)@P1, e) 10 wt.% NH_2-MIL-53(Al)@P2 and f) 10 wt.% NH_2-MIL-101(Al)@P2.

Figure 4. FTIR spectra during activation process for a) NH_2-MIL-53(Al). b) NH_2-MIL-101(Al).

Figure 5. Characterization of activated NH_2-MIL-53(Al) and NH_2-MIL-101(Al): a) TGA and DTG, b) N_2 adsorption/desorption isotherms at 77 K (solid symbols = adsorption; empty symbols = desorption).

Figure 6. DTG curves for MMMs: a) Polymer P1. b) Polymer P2.

Figure 7. ATR-FTIR spectra between 1850 and 1000 cm^{-1} for a) NH_2-MIL-53(Al), P1 and 5, 10 and 15 wt.% NH_2-MIL-53(Al)@P1 MMMs and b) NH_2-MIL-101(Al), P1 and 5 and 10 wt.% NH_2-MIL-101(Al)@P1 MMMs.

Figure 8. FITR spectra between 3800 and 3200 cm^{-1} for a) NH_2-MIL-53(Al) and 15 wt.% NH_2-MIL-53(Al)@P1 MMM subtracted the polymer P1 and b) NH_2-MIL-101(Al) and 10 wt.% NH_2-MIL-101(Al)@P1 MMM subtracted the polymer P1.

Figure 9. CO_2 permeability and CO_2/CH_4 ideal selectivity at 35 ºC and 3 bar as a function of MOF loading.

Figure 10. H_2 permeability and H_2/CH_4 ideal selectivity at 35 ºC and 3 bar as a function of MOF loading.

Figure 11. Robeson plot containing the MOF-MMMs reported in the literature (table 2) and the results obtained in this work: a) CO_2/CH_4 b) H_2/CH_4.

FIGURE 1

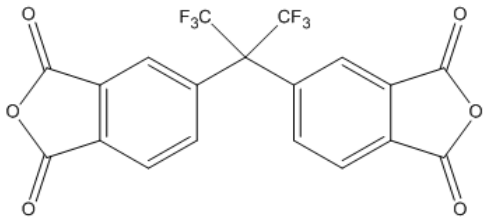

4,4’-(Hexafluoroisopropylidene)diphthalic dianhydride (6FDA)

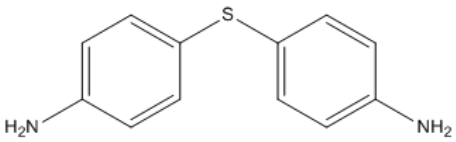

4,4’-Diaminodiphenyl sulfide (4,4`-SDA)

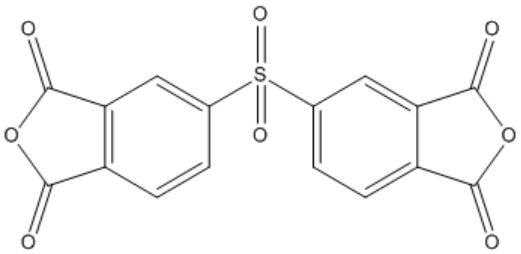

3,3’,4,4’-Diphenylsulfonetetracarboxylic dianydride (DSDA)

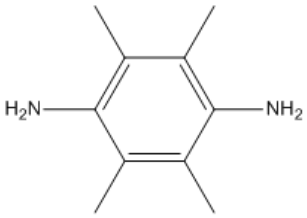

2,3,5,6-tetramethyl-1,4phenylene diamine (4MPD)

FIGURE 2

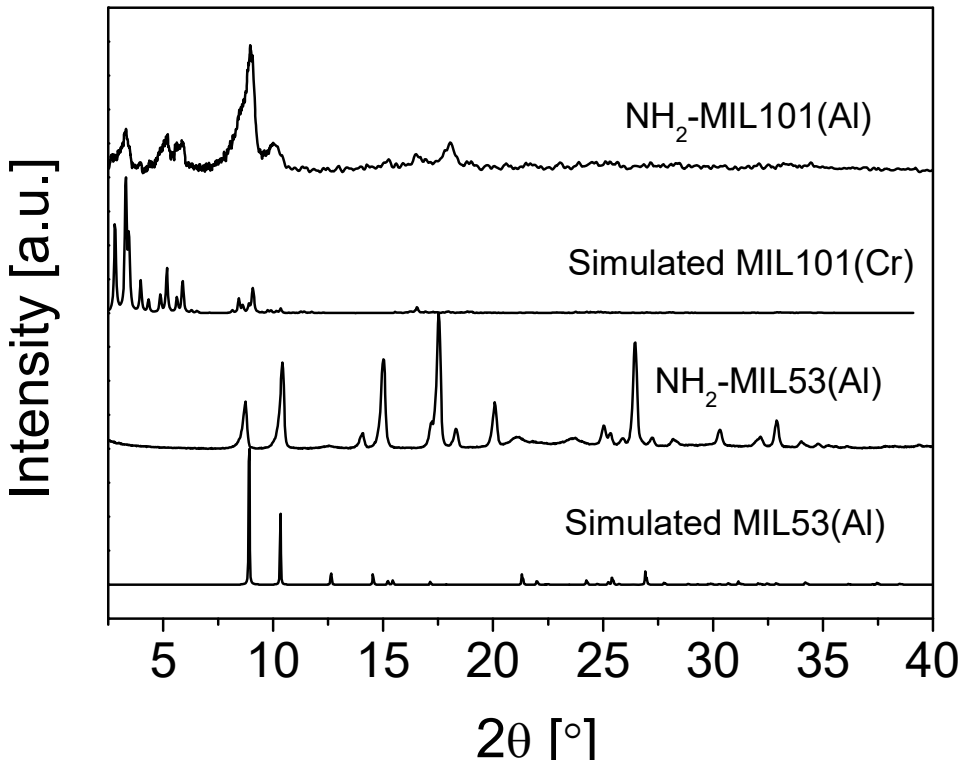
NH2-MIL101(Al)
Simulated MIL101(Cr)
NH2-MIL53(Al)
Simulated MIL53(Al)
Intensity [a.u.]
5
10
15
20
25
30
35
40
2θ [°]

FIGURE 3

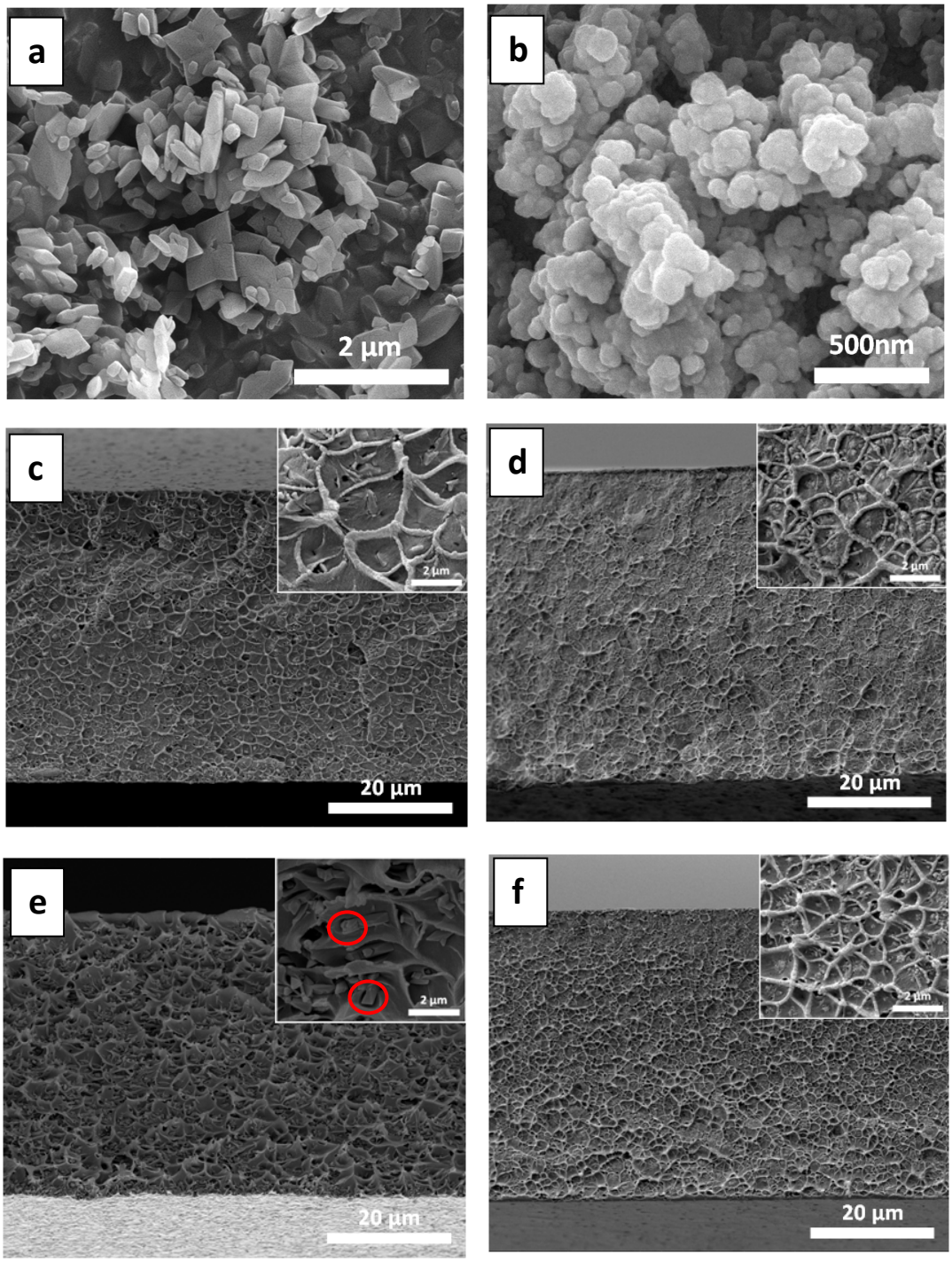

FIGURE 4

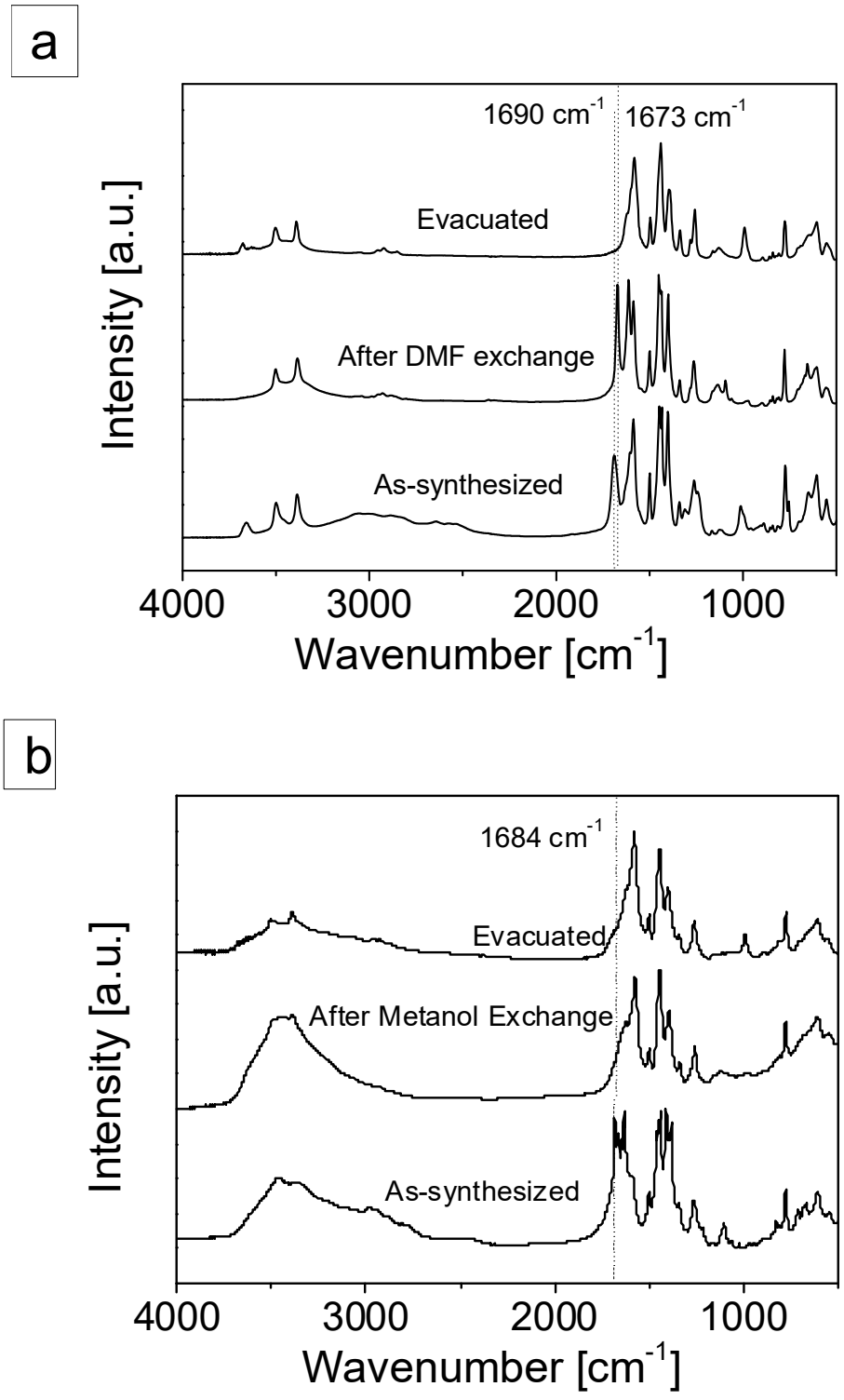
a
1690 cm-1
1673 cm-1
Evacuated
After DMF exchange
As-synthesized
Intensity [a.u.]
4000
3000
2000
1000
Wavenumber [cm-1]
b
1684 cm-1
Evacuated
After Metanol Exchange
As-synthesized
Intensity [a.u.]
4000
3000
2000
1000
Wavenumber [cm-1]

FIGURE 5

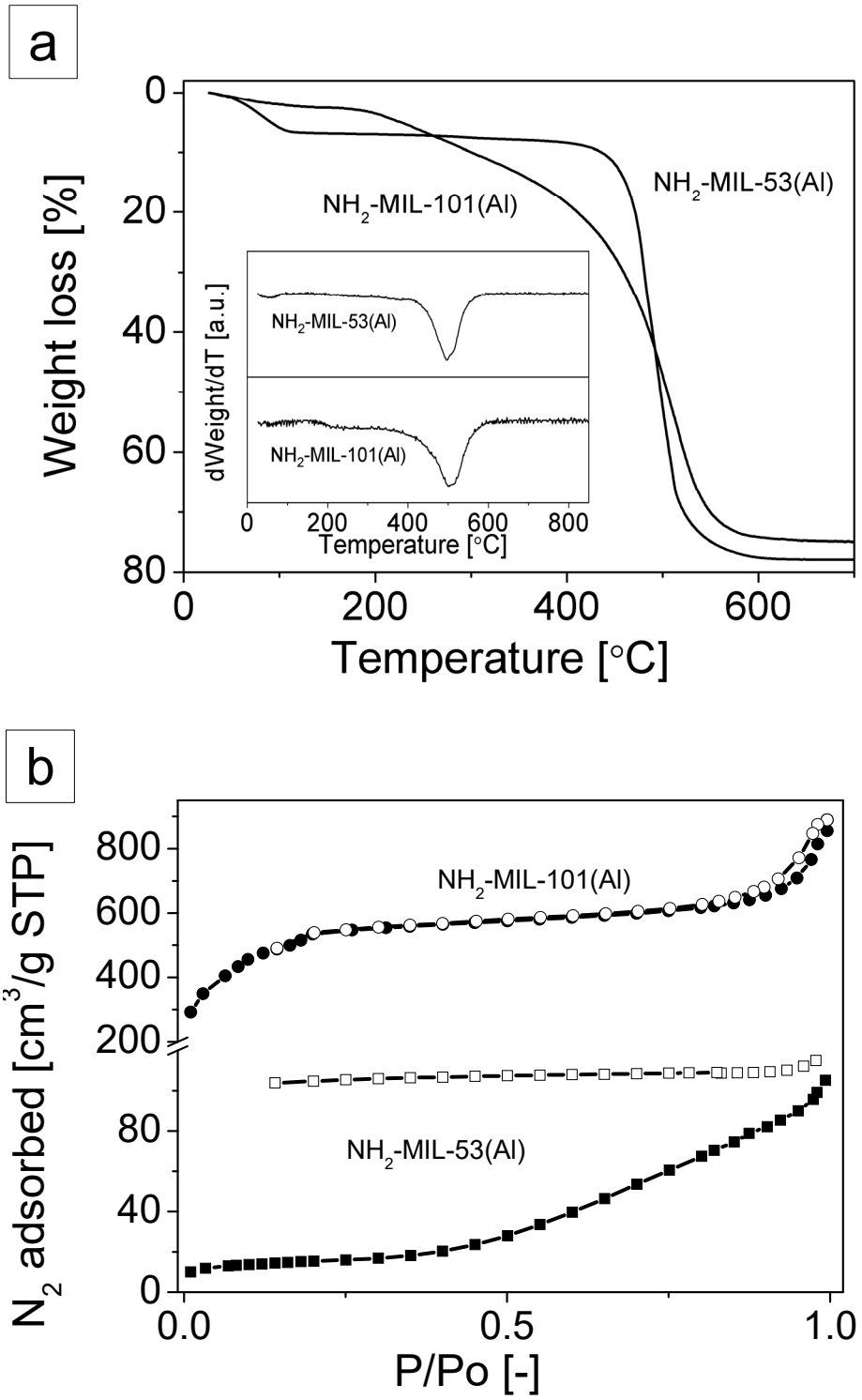
a
Weight loss [%]
Temperature [°C]
NH2-MIL-101(Al)
NH2-MIL-53(Al)
dWeight/dT [a.u.]
b
N2 adsorbed [cm3/g STP]
P/Po [-]
NH2-MIL-101(Al)
NH2-MIL-53(Al)

.

FIGURE 6

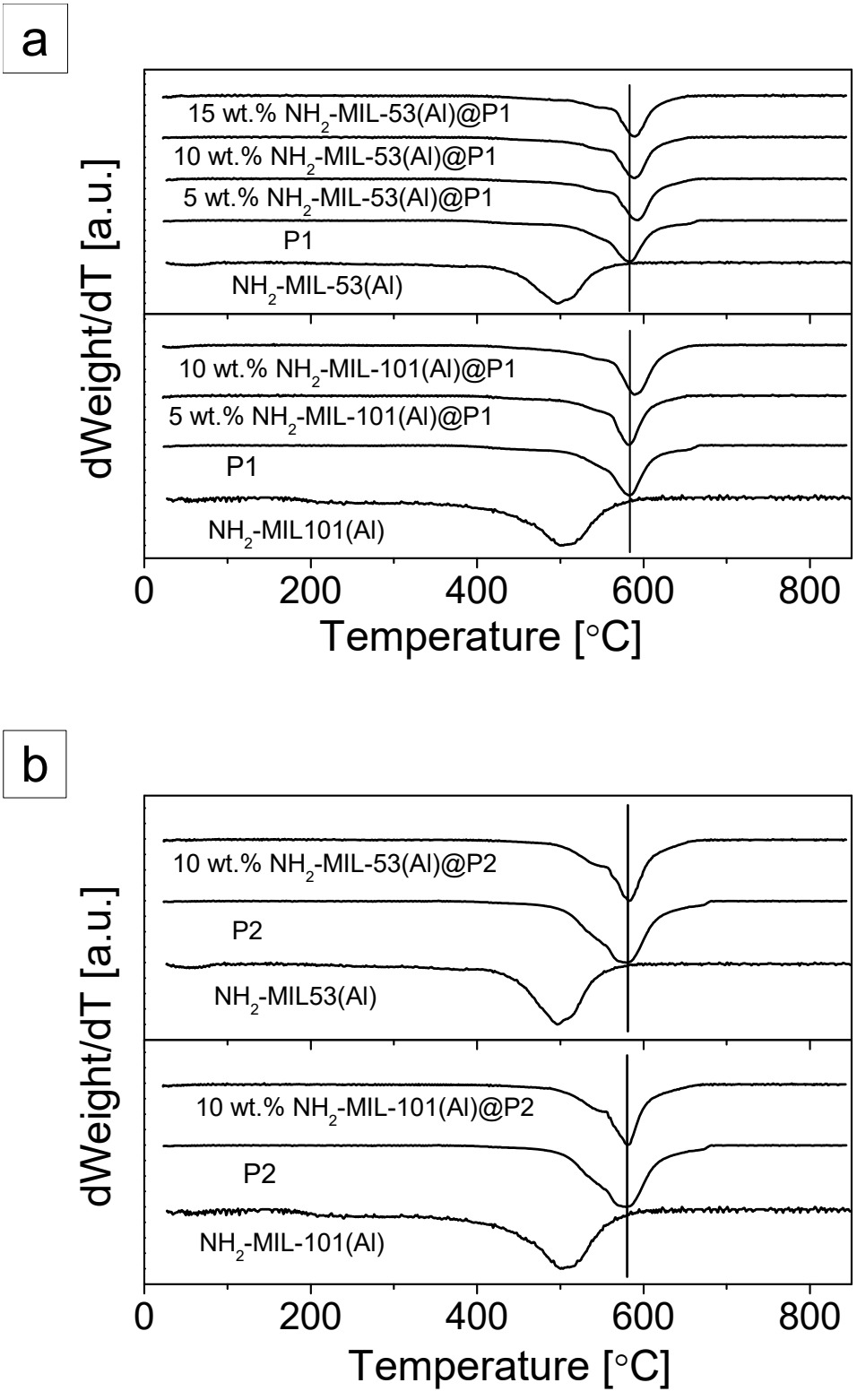
a
15 wt.% NH2-MIL-53(Al)@P1
10 wt.% NH2-MIL-53(Al)@P1
5 wt.% NH2-MIL-53(Al)@P1
P1
NH2-MIL-53(Al)
10 wt.% NH2-MIL-101(Al)@P1
5 wt.% NH2-MIL-101(Al)@P1
P1
NH2-MIL101(Al)
dWeight/dT [a.u.]
0
200
400
600
800
Temperature [°C]
b
10 wt.% NH2-MIL-53(Al)@P2
P2
NH2-MIL53(Al)
10 wt.% NH2-MIL-101(Al)@P2
P2
NH2-MIL-101(Al)
dWeight/dT [a.u.]
0
200
400
600
800
Temperature [°C]

FIGURE 7

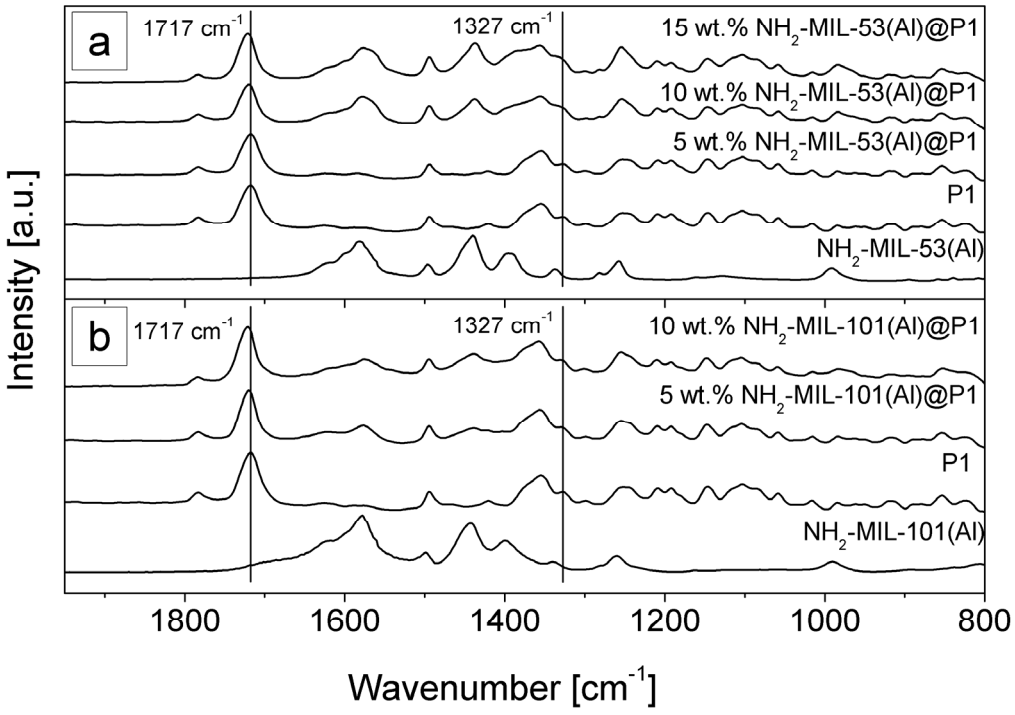
a
1717 cm-1
1327 cm-1
15 wt.% NH2-MIL-53(Al)@P1
10 wt.% NH2-MIL-53(Al)@P1
5 wt.% NH2-MIL-53(Al)@P1
P1
NH2-MIL-53(Al)
b
1717 cm-1
1327 cm-1
10 wt.% NH2-MIL-101(Al)@P1
5 wt.% NH2-MIL-101(Al)@P1
P1
NH2-MIL-101(Al)
Intensity [a.u.]
1800
1600
1400
1200
1000
800
Wavenumber [cm-1]

FIGURE 8

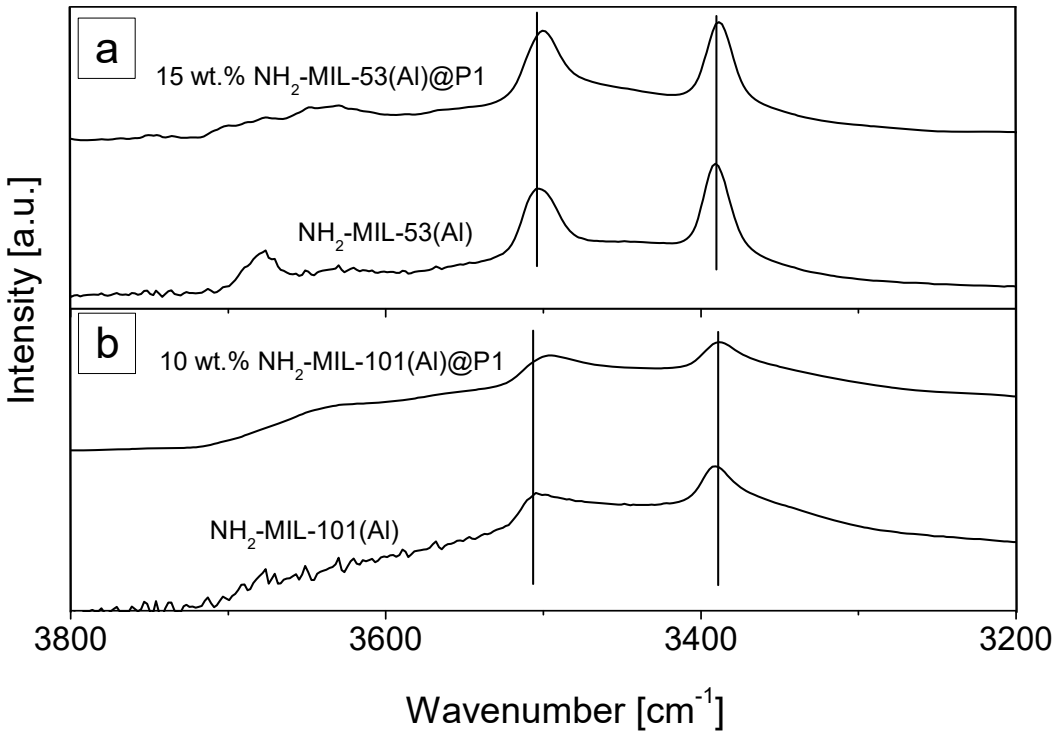
a
15 wt.% NH2-MIL-53(Al)@P1
NH2-MIL-53(Al)
b
10 wt.% NH2-MIL-101(Al)@P1
NH2-MIL-101(Al)
Intensity [a.u.]
3800
3600
3400
3200
Wavenumber [cm-1]

FIGURE 9

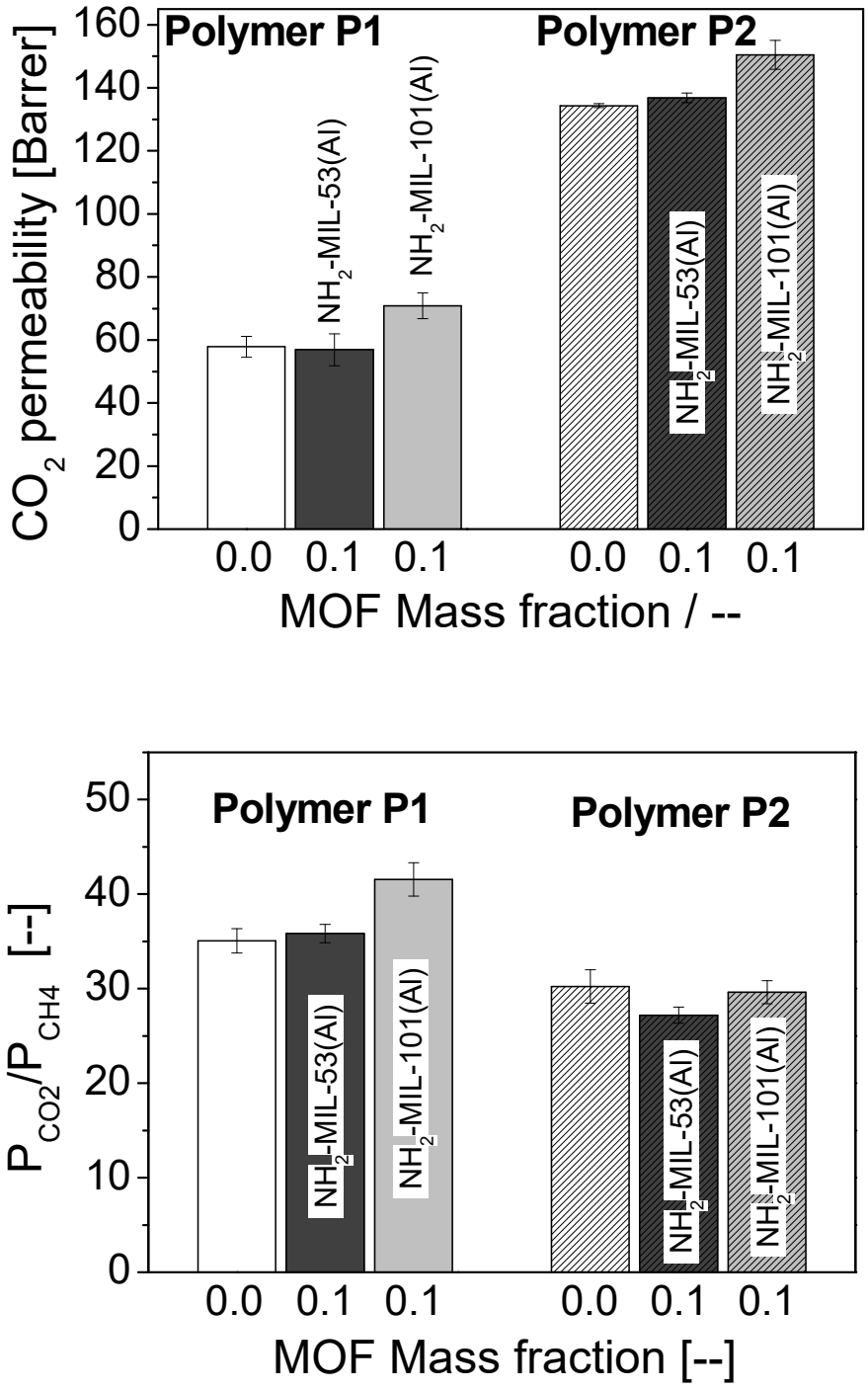
Polymer P1
Polymer P2
CO_2 permeability [Barrer]
160
140
120
100
80
60
40
20
0
NH_2-MIL-53(Al)
NH_2-MIL-101(Al)
0.0
0.1
0.1
0.0
0.1
0.1
MOF Mass fraction / --
P_{CO2}/P_{CH4} [--]
50
40
30
20
10
0
MOF Mass fraction [--]

FIGURE 10

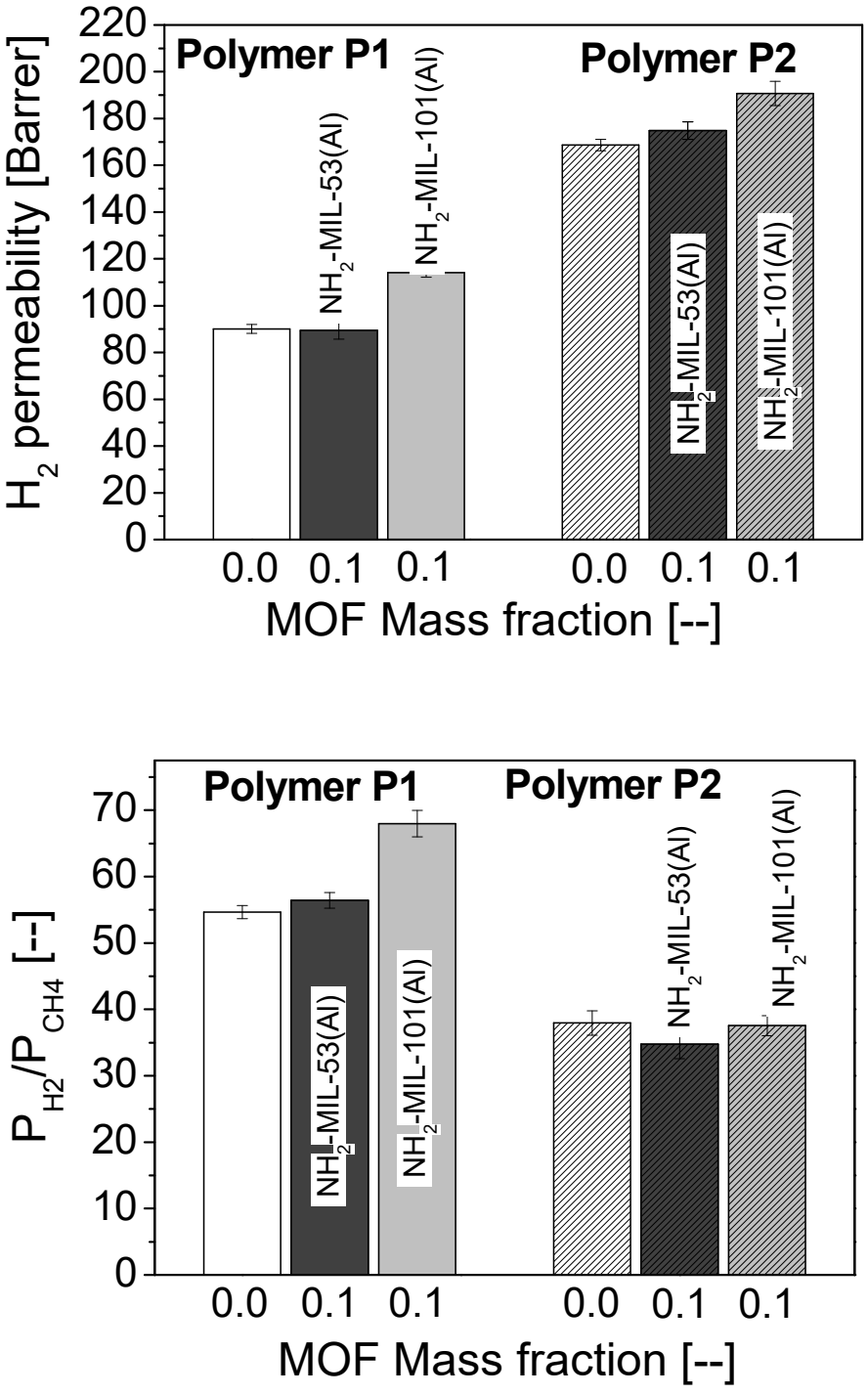
Polymer P1
Polymer P2
NH2-MIL-53(Al)
NH2-MIL-101(Al)
H2 permeability [Barrer]
0
20
40
60
80
100
120
140
160
180
200
220
0.0
0.1
0.1
0.0
0.1
0.1
MOF Mass fraction [--]
Polymer P1
Polymer P2
NH2-MIL-53(Al)
NH2-MIL-101(Al)
P H2/P CH4 [--]
0
10
20
30
40
50
60
70
0.0
0.1
0.1
0.0
0.1
0.1
MOF Mass fraction [--]

FIGURE 11

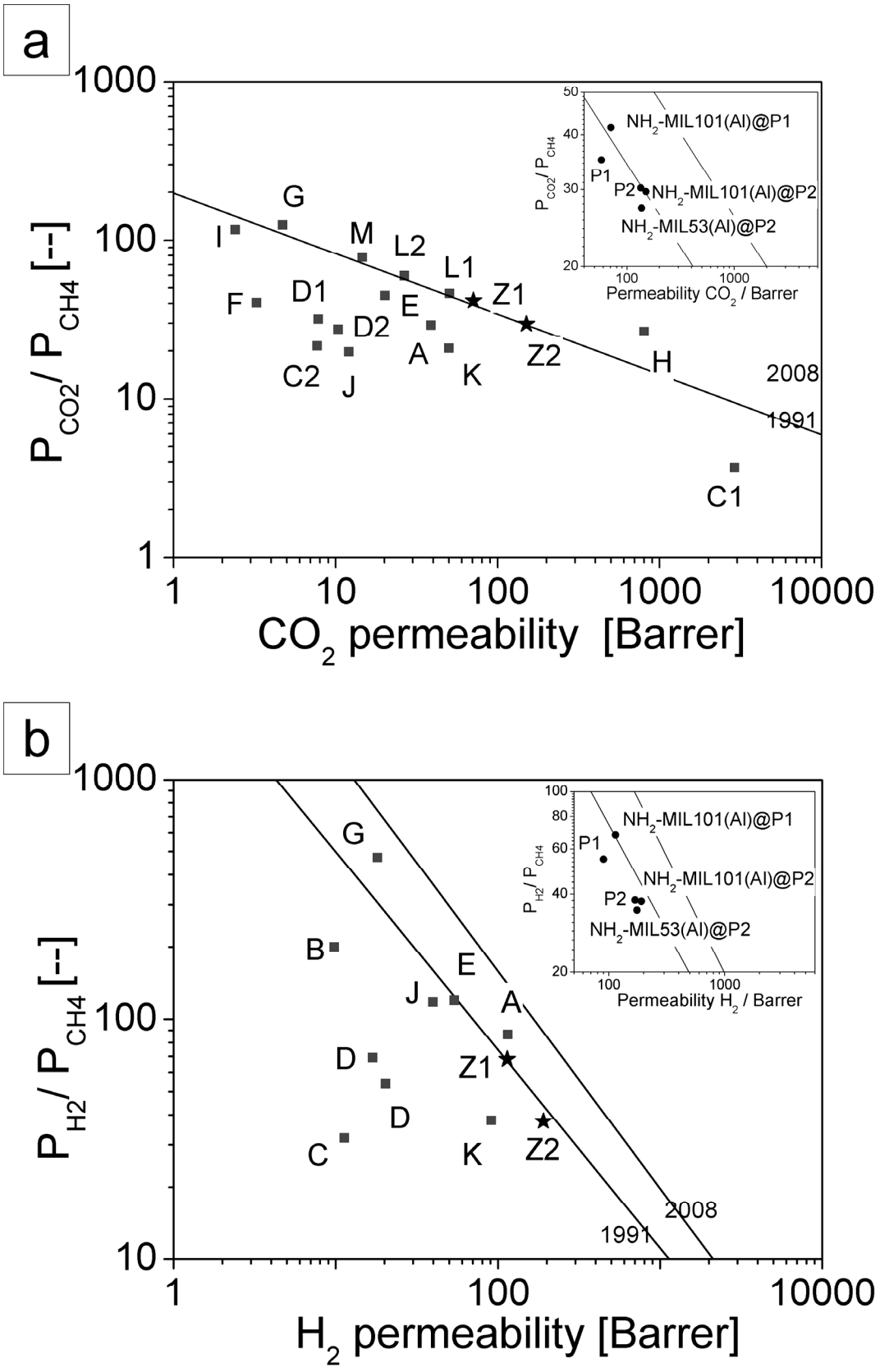
a
1000
100
10
1
P_{CO2} / P_{CH4} [--]
G
I
M
L2
L1
F
D1
E
Z1
D2
A
Z2
H
C2
J
K
2008
1991
C1
1
10
100
1000
10000
CO_2 permeability [Barrer]
50
40
30
20
P_{CO2} / P_{CH4}
NH_2-MIL101(Al)@P1
P1
P2
NH_2-MIL101(Al)@P2
NH_2-MIL53(Al)@P2
100
1000
Permeability CO_2 / Barrer
b
1000
100
10
P_{H2} / P_{CH4} [--]
G
B
E
J
A
D
Z1
D
C
K
Z2
2008
1991
1
100
10000
H_2 permeability [Barrer]
100
80
60
40
20
P_{H2} / P_{CH4}
NH_2-MIL101(Al)@P1
P1
NH_2-MIL101(Al)@P2
P2
NH_2-MIL53(Al)@P2
100
1000
Permeability H_2 / Barrer

References

[1] J.C. Davis, R.J. Valus, R. Eshraghi, A.E. Velikoff, Facilitated transport membrane hybrid systems for olefin purification, Sep. Sci. Technol. 28 (1993) 463-476.

[2] J. Gascon, F. Kapteijn, B. Zornoza, V. Sebastian, C. Casado, J. Coronas, Practical approach to zeolitic membranes and coatings: State of the art, opportunities, barriers, and future perspectives, Chem. Mater. 24 (2012) 2829-2844.

[3] L.M. Robeson, Correlation of separation factor versus permeability for polymeric membranes, J. Membr. Sci. 62 (1991) 165-185.

[4] L.M. Robeson, The upper bound revisited, J. Membr. Sci. 320 (2008) 390-400.

[5] T.S. Chung, L.Y. Jiang, Y. Li, S. Kulprathipanja, Mixed matrix membranes (MMMs) comprising organic polymers with dispersed inorganic fillers for gas separation, Prog. Polym. Sci. 32 (2007) 483-507.

[6] P.S. Goh, A.F. Ismail, S.M. Sanip, B.C. Ng, M. Aziz, Recent advances of inorganic fillers in mixed matrix membrane for gas separation, Sep. Purif. Technol. 81 (2011) 243-264.

[7] B. Zornoza, C. Tellez, J. Coronas, J. Gascon, F. Kapteijn, Metal organic framework based mixed matrix membranes: An increasingly important field of research with a large application potential, Microporous and Mesoporous Mater. (2013) 67-68.

[8] T.T. Moore, W.J. Koros, Non-ideal effects in organic-inorganic materials for gas separation membranes, J. Mol. Struct. 739 (2005) 87-98.

[9] K.K. Tanabe, S.M. Cohen, Postsynthetic modification of metal-organic frameworks-a progress report, Chem. Soc. Rev. 40 (2011) 498-519.

[10] M. Eddaoudi, J. Kim, N. Rosi, D. Vodak, J. Wachter, M. O'Keeffe, O.M. Yaghi, Systematic design of pore size and functionality in isoreticular MOFs and their application in methane storage, Science 295 (2002) 469-472.

[11] H. Yehia, T.J. Pisklak, J.P. Ferraris, K.J. Balkus, I.H. Musselman, Methane facilitated transport using copper(II) biphenyl dicarboxylate-triethylenediamine/poly(3-acetoxyethylthiophene) mixed matrix membranes, Abstr. Paper Am. Chem. Soc. 227 (2004) U351-U351.

[12] H.B. Tanh Jeazet, C. Staudt, C. Janiak, Metal-organic frameworks in mixed-matrix membranes for gas separation, Dalton Trans. 41 (2012) 14003-14027.

[13] K. Hunger, N. Schmeling, H.B. Tanh Jeazet, C. Janiak, C. Staudt, K. Kleinermanns, Investigation of cross-linked and additive containing polymer materials for membranes with improved performance in pervaporation and gas separation, Membranes. 2 (2012) 727-763.

[14] T.H. Bae, J.S. Lee, W.L. Qiu, W.J. Koros, C.W. Jones, S. Nair, A high-performance gas-separation membrane containing submicrometer-sized metal-organic framework crystals, Angew. Chem., Int. Ed. 49 (2010) 9863-9866.

[15] B. Zornoza, A. Martinez-Joaristi, P. Serra-Crespo, C. Tellez, J. Coronas, J. Gascon, F. Kapteijn, Functionalized flexible MOFs as fillers in mixed matrix membranes for highly selective separation of CO_2 from CH_4 at elevated pressures, Chem. Commun. 47 (2011) 9522-9524.

[16] X.Y. Chen, H. Vinh-Thang, D. Rodrigue, S. Kaliaguine, Amine-functionalized MIL-53 metal-organic framework in polyimide mixed matrix membranes for CO_2/CH_4 separation, Ind. Eng. Chem. Res. 51 (2012) 6895-6906.

[17] O.G. Nik, X.Y. Chen, S. Kaliaguine, Functionalized metal organic framework-polyimide mixed matrix membranes for CO_2/CH_4 separation, J. Membr. Sci. 413 (2012) 48-61.

[18] B. Arstad, H. Fjellvag, K.O. Kongshaug, O. Swang, R. Blom, Amine functionalised metal organic frameworks (MOFs) as adsorbents for carbon dioxide, Adsorption 14 (2008) 755-762.
[19] T. Loiseau, C. Serre, C. Huguenard, G. Fink, F. Taulelle, M. Henry, T. Bataille, G. Ferey, A rationale for the large breathing of the porous aluminum terephthalate (MIL-53) upon hydration, Chem. Eur. J. 10 (2004) 1373-1382.
[20] T. Ahnfeldt, D. Gunzelmann, T. Loiseau, D. Hirsemann, J. Senker, G. Ferey, N. Stock, Synthesis and modification of a functionalized 3D open-framework structure with MIL-53 topology, Inorg. Chem. 48 (2009) 3057-3064.
[21] S. Couck, E. Gobechiya, C.E.A. Kirschhock, P. Serra-Crespo, J. Juan-Alcaniz, A.M. Joaristi, E. Stavitski, J. Gascon, F. Kapteijn, G.V. Baron, J.F.M. Denayer, Adsorption and separation of light gases on an amino-functionalized metal-organic framework: An adsorption and in situ XRD study, ChemSusChem 5 (2012) 740-750.
[22] E. Stavitski, M. Goesten, J. Juan-Alcaniz, A. Martinez-Joaristi, P. Serra-Crespo, A.V. Petukhov, J. Gascon, F. Kapteijn, Kinetic control of metal-organic framework crystallization investigated by time-resolved in situ X-ray scattering, Angew. Chem., Int. Ed. 50 (2011) 9624-9628.
[23] G. Ferey, C. Mellot-Draznieks, C. Serre, F. Millange, J. Dutour, S. Surble, I. Margiolaki, A chromium terephthalate-based solid with unusually large pore volumes and surface area, Science 309 (2005) 2040-2042.
[24] P. Serra-Crespo, E.V. Ramos-Fernandez, J. Gascon, F. Kapteijn, Synthesis and characterization of an amino functionalized MIL-101(Al): separation and catalytic properties, Chem. Mater. 23 (2011) 2565-2572.
[25] D. Duesselberg, D. Verreault, P. Koelsch, C. Staudt, Synthesis and characterization of novel, soluble sulfur-containing copolyimides with high refractive indices, J. Mater. Sci. 46 (2011) 4872-4879.
[26] J.U. Wieneke, C. Staudt, Thermal stability of 6FDA-(co-)polyimides containing carboxylic acid groups, Polym. Degrad. Stab. 95 (2010) 684-693.
[27] R. Adams, C. Carson, J. Ward, R. Tannenbaum, W. Koros, Metal organic framework mixed matrix membranes for gas separations, Microporous and Mesoporous Mater. 131 (2010) 13-20.
[28] C. Serre, F. Millange, C. Thouvenot, M. Nogues, G. Marsolier, D. Louer, G. Ferey, Very large breathing effect in the first nanoporous $Cr^{III}(OH)\cdot\{O_2C\text{-}C_6H_4\text{-}CO_2\}\cdot\{HO_2C\text{-}C_6H_4\text{-}CO_2H\}_x\cdot H_2O_y$, J. Am. Chem. Soc. 124 (2002) 13519-13526.
[29] K.S. Walton, R.Q. Snurr, Applicability of the BET method for determining surface areas of microporous metal-organic frameworks, J. Am. Chem. Soc. 129 (2007) 8552-8556.
[30] H. Ren, J. Jin, J. Hu, H. Liu, Affinity between metal-organic frameworks and polyimides in asymmetric mixed matrix membranes for gas separations, Ind. Eng. Chem. Res. 51 (2012) 10156-10164.
[31] Y.F. Zhang, I.H. Musseman, J.P. Ferraris, K.J. Balkus, Gas permeability properties of Matrimid (R) membranes containing the metal-organic framework Cu-BPY-HFS, J. Membr. Sci. 313 (2008) 170-181.
[32] E.V. Perez, K.J. Balkus, J.P. Ferraris, I.H. Musselman, Mixed-matrix membranes containing MOF-5 for gas separations, J. Membr. Sci. 328 (2009) 165-173.
[33] M. Mrsevic, D. Duesselberg, C. Staudt, Synthesis and characterization of a novel carboxyl group containing (co)polyimide with sulfur in the polymer backbone, Beilstein J. Org. Chem. 8 (2012) 776-786.

[34] S.I. Kim, T.J. Shin, M. Ree, H. Lee, T. Chang, C. Lee, T.H. Woo, S.B. Rhee, Structure and properties of various poly(amic diisopropyl ester-alt-imide)s and their alternating copolyimides, Polymer 41 (2000) 5173-5184.
[35] S.D. Xiao, X.S. Feng, R.Y.M. Huang, Synthetic 6FDA-ODA copolyimide membranes for gas separation and pervaporation: Correlation of separation properties with diamine monomers, Polym. Eng. Sci. 48 (2008) 795-805.
[36] K. Tanaka, H. Kita, M. Okano, K. Okamoto, Permeability and permselectivity of gases in fluorinated and non-fluorinated polyimides, Polymer 33 (1992) 585-592.
[37] S.L. Liu, R. Wang, T.S. Chung, M.L. Chng, Y. Liu, R.H. Vora, Effect of diamine composition on the gas transport properties in 6FDA-durene/3,3 '-diaminodiphenyl sulfone copolyimides, J. Membr. Sci. 202 (2002) 165-176.
[38] F. Zhang, X. Zou, X. Gao, S. Fan, F. Sun, H. Ren, G. Zhu, Hydrogen selective NH_2-MIL-53(Al) MOF membranes with high permeability, Adv. Funct. Mater. 22 (2012) 3583-3590.
[39] H.B.T. Jeazet, C. Staudt, C. Janiak, A method for increasing permeability in O_2/N_2 separation with mixed-matrix membranes made of water-stable MIL-101 and polysulfone, Chem. Commun. 48 (2012) 2140-2142.
[40] S. Couck, J.F.M. Denayer, G.V. Baron, T. Remy, J. Gascon, F. Kapteijn, An amine-functionalized MIL-53 metal-organic framework with large separation power for CO_2 and CH_4, J. Am. Chem. Soc. 131 (2009) 6326-3627.
[41] C. Liu, B. McCulloch, S.T. Wilson, A.I. Benin, M.E. Schott, US 7637983, 2009.
[42] J.G. Won, J.S. Seo, J.H. Kim, H.S. Kim, Y.S. Kang, S.J. Kim, Y.M. Kim, J.G. Jegal, Coordination compound molecular sieve membranes, Adv. Mater. 17 (2005) 80-84.
[43] A. Car, C. Stropnik, K.V. Peinemann, Hybrid membrane materials with different metal-organic frameworks (MOFs) for gas separation, Desalination 200 (2006) 424-426.
[44] M.J.C. Ordonez, K.J. Balkus, Jr., J.P. Ferraris, I.H. Musselman, Molecular sieving realized with ZIF-8/Matrimid (R) mixed-matrix membranes, J. Membr. Sci. 361 (2010) 28-37.
[45] B. Zornoza, B. Seoane, J.M. Zamaro, C. Tellez, J. Coronas, Combination of MOFs and zeolites for mixed-matrix membranes, ChemPhysChem 12 (2011) 2781-2785.
[46] K. Diaz, M. Lopez-Gonzalez, L.F. del Castillo, E. Riande, Effect of zeolitic imidazolate frameworks on the gas transport performance of ZIF8-poly(1,4-phenylene ether-ether-sulfone) hybrid membranes, J. Membr. Sci. 383 (2011) 206-213.
[47] S. Basu, A. Cano-Odena, I. F. J. Vankelecom, MOF-containing mixed matrix membranes for CO_2/CH_4 and CO_2/N_2 binary gas mixture separations, Sep. Purif. Technol. 81 (2011) 31-40.